

Dynamic and Heat Effects in Sinusoidal Surface DBD

V.A. Bituryn and A.N. Bocharov

Joint Institute for High Temperatures of Russian Academy of Sciences, Izhorskaya str.
13, Bld. 2, Moscow, Russia

valentin.bituryn@gmail.com

Abstract. Numerical simulation of sinusoidal Surface Dielectric Barrier Discharge (SDBD) is carried out. The configuration and parameters of the discharge are those considered experimentally in paper [1]. In this paper, dielectric disc was surrounded by high-voltage metallic electrode. 34 kHz 5.5 kV applied to HV electrode at atmospheric pressure. The objective of the current paper is to study mechanisms inducing flow motion over the disc. Numerical simulations are made with the two-dimensional model developed earlier in paper [2]. The model incorporates the transport of charged particles, Poisson equation for the electric field strength, and Navier-Stokes equations for the fluid. In addition to the bulk processes (mainly, ionization, recombination, drift and diffusion) the deposition of the charge on the dielectric surface is considered.

1. Computational model for pulse-periodic discharge

The problem setup simulates, in general, the discharge studied in paper [1]. The pulse-periodic discharge over the disc dielectric plate surrounded with annular high-voltage (HV) electrode is considered. The diameter of dielectric disc was taken to be 14 mm. External diameter of HV electrode was taken to be 24 mm. The diameter of the grounded electrode is assumed to be the same as the dielectric one. Thickness of dielectric was taken as 0.3 mm; dielectric permeability is equal to 3. Sinusoidal 5.5kV voltage is applied to HV electrode with the frequency 33.3 kHz in air at atmospheric pressure. The discharge domain considered below is presented in Fig. 1.

The computational model is basically same as those described in paper [2,3]. We assume that the flow and electric discharge characteristics can be described by the set of equations reflecting conservation of mass, momentum and total energy for the whole fluid. Transport equations for charged particles, electrons and ions, as well as the Poisson equation for the electric field strength are solved assuming the drift-diffusion approach is valid. The set of governing equations is given below.

$$\frac{\partial \rho}{\partial t} + (\rho \mathbf{U}) = 0 \quad (1)$$

$$\frac{\partial \rho \mathbf{U}}{\partial t} + (\rho \mathbf{U} \mathbf{U}) + \nabla \tau = \frac{\partial P}{\partial \mathbf{r}} \quad (2)$$

$$\frac{\partial \rho E}{\partial t} + (\rho \mathbf{U} H) + \nabla (\mathbf{U} \tau) + \nabla \mathbf{q} = 0 \quad (3)$$

Here, ρ is the density, $\mathbf{U} = (U_x, U_y)$ is velocity, P is the thermodynamic pressure, E is specific total energy, H is specific total enthalpy.



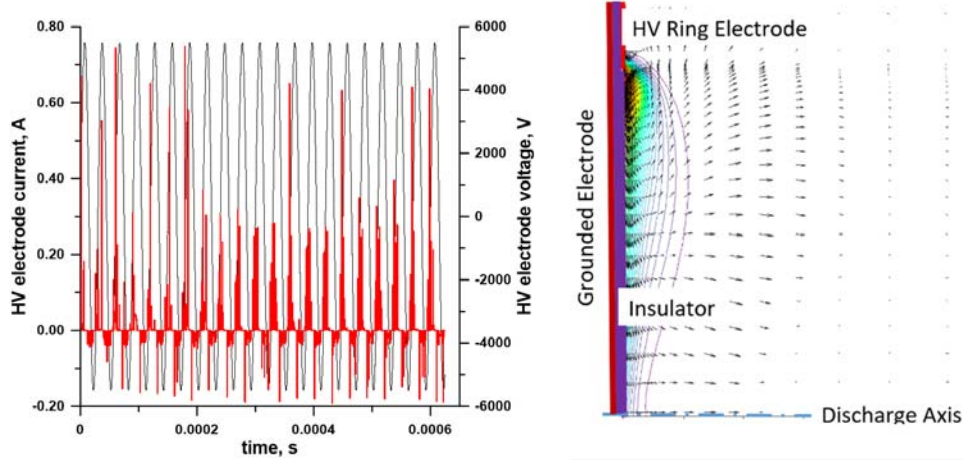


Fig.1 The time dependents of the HV electrode current (red line) and voltage (black line) at 34kHz 5.5kV SDBD (left) and temperature (colored lines) and velocity-vectors after 20 cycles. $T_{\max}=674\text{K}$, $V_{\max}=0.88\text{m/s}$ (right).

$$H = E + \frac{P}{\rho}, E = e + \frac{U^2}{2}, (\gamma - 1)e = P/\rho, P = \rho R T \quad (4)$$

Here, $\gamma = 1.4$ is the ratio of specific heats, and T is the temperature. Viscous stress tensor components and heat fluxes are specified as usually:

$$\tau_{ij} = \frac{2}{3}\eta\delta_{ij}\nabla\mathbf{U} - \eta\left(\frac{\partial U_i}{\partial x_j} + \frac{\partial U_j}{\partial x_i}\right), \mathbf{q} = -\lambda\frac{\partial T}{\partial \mathbf{r}} \quad (5)$$

where δ_{ij} is Kronecker symbol, η is viscosity, λ is heat conductivity. Gradient and divergence operators are defined as follows:

$$\frac{\partial}{\partial \mathbf{r}} = \mathbf{e}_x \frac{\partial}{\partial x} + \mathbf{e}_y \frac{\partial}{\partial y}, \nabla = \frac{\partial}{\partial x} + \frac{1}{y^\xi} \frac{\partial}{\partial y} y^\xi, \quad (6)$$

Where \mathbf{e}_x and \mathbf{e}_y are unit base-vectors, $\xi=0$ for Cartesian coordinate system, and $\xi=1$ for axi-symmetric one.

The transport equations for concentrations and Poisson equation for electric field are read as follows:

$$\frac{\partial n_i}{\partial t} + \nabla \Gamma_i = \dot{Q} \quad (7)$$

$$\frac{\partial n_e}{\partial t} + \nabla \Gamma_e = \dot{Q} \quad (8)$$

$$\varepsilon \nabla \mathbf{E} = \rho_e, \rho_e = q(n_i - n_e) \quad (9)$$

In Eqs. (7) through (9) n_i is ion number density, n_e is electron number density, ρ_e is the electric charge density, \mathbf{E} is electric field, $\mathbf{E} = -\frac{\partial \varphi}{\partial \mathbf{r}}$, φ is the electric potential, q is electron charge, ε is permittivity of vacuum, \dot{Q} is the source term defined later. Strictly speaking the Poisson equation with zero right-hand-side should also be solved in the bulk of dielectric. In this paper, simplified approach is used. Namely, the dielectric surface is considered via special boundary conditions on the plasma-dielectric boundary.

Ion and electron fluxes, Γ_i and Γ_e , are defined as follows

$$\Gamma_i = n_i(\mathbf{U} + \mathbf{V}_{di}) - D_i \frac{\partial n_i}{\partial \mathbf{r}}$$

$$\mathbf{\Gamma}_e = n_e(\mathbf{U} + \mathbf{V}_{de}) - D_e \frac{\partial n_e}{\partial r} \quad (10)$$

Here, drift velocities \mathbf{V}_{di} and \mathbf{V}_{de} are defined as

$$\mathbf{V}_{di} = \mu_i \mathbf{E}, \mathbf{V}_{de} = -\mu_e \mathbf{E} \quad (11)$$

where μ_i and μ_e are ion and electron mobilities, respectively:

$$\mu_{i,e} = \frac{q/m_{i,e}}{v_{i,e}}, v_{i,e} = \frac{2\sqrt{2}}{3} \pi d_{i,e}^2 \left(\frac{8kT_{i,e}}{\pi m_{i,e}} \right)^{1/2} \quad (12)$$

In (12) $d_{i,e}$ are mean collision cross-section diameters for ions and electrons, respectively. T_i and T_e are ion and electron temperature, respectively. m_i and m_e are ion and electron mass. $v_{i,e}$ are mean collision frequencies for ion-neutral and electron-neutral collisions.

Diffusion coefficients, D_i and D_e in (10) are defined as

$$D_i = \mu_i k_B T_i / q, D_e = \mu_e k_B T_e / q \quad (13)$$

In (13) k_B is the Boltzman's constant. In paper [2] we used an approximation for electron temperature as function of the reduced electric field, $E_r = E/n$ (Td), where $n = P/k_B T$ is the total number density. Here, we simply take $T_e = 2\text{eV}$, and $T_i = T$.

Electric current density is determined as

$$\mathbf{j} = \mathbf{j}_i + \mathbf{j}_e = q(\mathbf{\Gamma}_i - \mathbf{\Gamma}_e)$$

Source-terms in equations (2), (3), (7) and (8) are determined as follows

$$\dot{F} = \rho_e E,$$

$$\dot{W} = \eta_e j_e E + \eta_i j_i E \quad (14)$$

$$\dot{Q} = \alpha n_e - \beta n_e n_i \quad (15)$$

The following approximations for ionization coefficient, α , and recombination coefficient, β , obtained with using Boltzman's solver³ are used in the paper [3]:

$$\alpha = 10^{-6} \cdot (0.79 K_1 + 0.21 K_2) \cdot n$$

$$K_1 = 8.9 \cdot 10^{-9} \exp(-927.7 / E_r), \text{ if } E_r < 300, K_1 = 4.27 \cdot 10^{-8} \exp(-927.7 / E_r), \text{ if } 300 < E_r < 1423,$$

$$K_1 = 10^{-10} \cdot (-110.67 + 21.8 E_r), \text{ otherwise.}$$

$$K_2 = 4.9 \cdot 10^{-9} \exp(-657.8 / E_r), \text{ if } E_r < 260, K_2 = 2.88 \cdot 10^{-8} \exp(-1118 / E_r) \cdot (1 + 4 \cdot 10^{-10} \cdot E_r^3),$$

$$\text{if } 260 < E_r < 1000,$$

$$K_2 = 10^{-10} \cdot (-110.67 + 21.8 E_r), \text{ otherwise.}$$

$$\beta = 2 \cdot 10^{-13} \cdot (300 / T_e)^{0.7}$$

First of terms (14) is the body force acting on the fluid. Second term is the heat from flowing electron and ion currents. It has been taken in this paper that, $\eta_e = 1$ and $\eta_i = 1$.

The boundary conditions for flow variables are specified as follows. No-slip adiabatic wall conditions are set on the surface of electrode and dielectric surface. Symmetry boundary conditions are set at the symmetry axis. Namely, $\mathbf{U} \cdot \mathbf{n} = 0$, $\partial/\partial n = 0$ for other variables. Here, \mathbf{n} – is the unit normal vector. Far-field boundary conditions are specified at other boundaries of the domain.

Boundary conditions for plasma variables are specified as follows. At symmetry axis zero normal gradients are set for n_e , n_i , and ϕ . At the outer boundary (except HV electrode and dielectric surfaces) zero normal gradients are also set for all plasma variables. At the electrode and dielectric surfaces, the type of boundary conditions depends on the operation mode of electrode. The latter is determined by the sign of the projection of electric field on to outer normal to the surface. If it is positive, anode-type boundary conditions are applied. Otherwise, cathode-type boundary conditions are used. Anode-type conditions are specified as follows. Zero normal gradient for the electron number density is set, as well

as zero ion number density. Boundary condition for electric potential is specified depending on the metallic or dielectric surface is considered. At the electrode surface potential is specified as: $\phi_{HV} = E(t) = E_0 \sin(2\pi\nu t)$, where $E_0 = 5.5\text{kV}$, $\nu = 33.3\text{kHz}$. Cathode-type boundary conditions are set as follows. Zero normal gradient is set for ion number density. Relation $(\Gamma_e \mathbf{n}) = -\gamma_e(\Gamma_i \mathbf{n})$ is used for electrons. In this relation, γ_e is coefficient of secondary electron emission. Calculations were carried out with $\gamma_e = 0.01$. Electric potential at the HV electrode is set as described above. At the dielectric surface, the jump condition for electric field strength projection is specified:

$$\varepsilon_P(\mathbf{E}_P \mathbf{n}) - \varepsilon_D(\mathbf{E}_D \mathbf{n}) + (1/q) \cdot \mathbf{j} \mathbf{n} dt = 0 \quad (16)$$

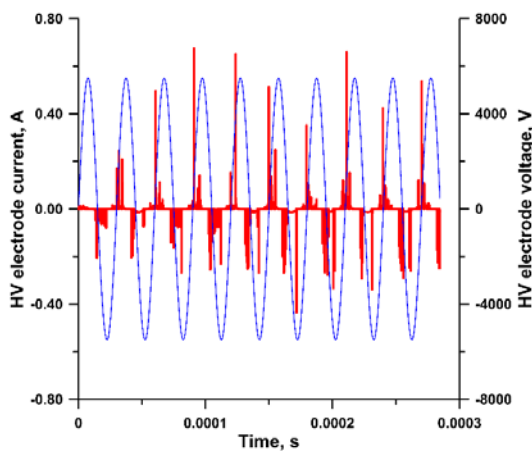


Fig.2. HV electrode current (red line) and voltage (blue line) vs time in interval (0 – 0.3) ms..

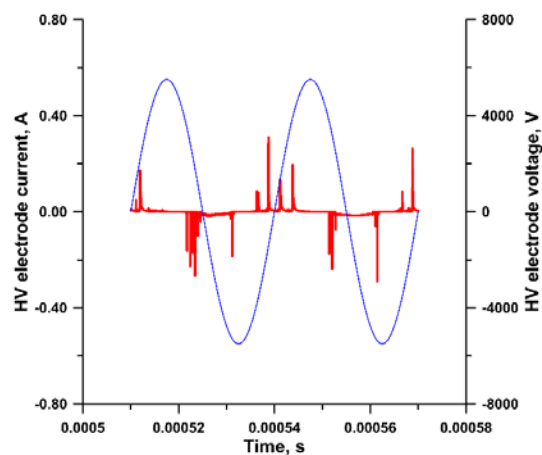


Fig.3. HV electrode current (red line) and voltage (blue line) vs time in interval (0.5 ms – 0.58) ms

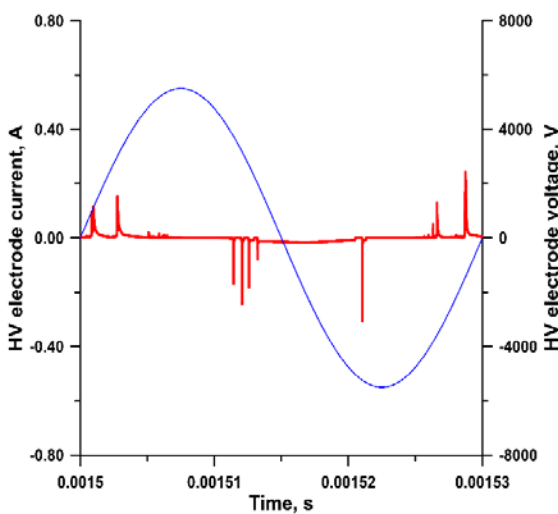


Fig.4. HV electrode current (red line) and voltage (blue line) vs time in interval 1.5 ms – 1.53) ms

Here, ε_P is electric permittivity of plasma, $\varepsilon_P = \varepsilon_0$. ε_D electric permittivity of dielectric material. In the paper $\varepsilon_D = 3\varepsilon_0$. $(\mathbf{E}_P \mathbf{n})$ is projection of electric field strength onto normal-to-surface from the side of plasma, and $(\mathbf{E}_D \mathbf{n})$ is projection of electric field from the side of dielectric. The latter term in (15) represents accumulation of the charge on the surface due to the flux of charged particles onto the surface. In general, equations (7) – (9) coupled with the equation for electric potential within the dielectric should be solved using conjugate condition (15) at the plasma-dielectric interface. In this paper simpler approach is used, in which the dielectric field strength, \mathbf{E}_D , is approximated as $(\mathbf{E}_D \mathbf{n}) = -(\phi_D - \phi_G)/\Delta$. Here, ϕ_D is the value of potential at the point of dielectric surface under consideration. ϕ_G is the potential of grounded metallic electrode built-in dielectric, $\phi_G = 0$. Δ is characteristic length scale, which, in general, is a function of surface coordinate. With this, relation (15) is a 3rd kind boundary condition for plasma region only and can be used for rough estimations of charge accumulation effect.

Initial state is specified as follows. Quiet (no flow) atmospheric air is assumed over the computational domain. Plasma sheet as thick as $50\text{ }\mu\text{m}$ with $n_e=n_i=10^{16}\text{ m}^{-3}$ is set over the surface.

To estimate long-term action of pulse-periodic discharge on the flow field special technique developed in paper³ is applied. Namely, the time-averaged source-terms (14) from equations (2) and (3) are used in time-integrating the Navier-Stokes equations. In turn, the time-averaged source-terms are computed while integrating the full set of equations during one or two cycles. Remind that the cycle time is $30\text{ }\mu\text{s}$, which is much smaller than characteristic hydrodynamic time of order of 10 ms .

2. Results and Discussion

Consider the characteristics of the discharge during one cycle. The HV electrode current vs time is represented in Fig.2 – Fig.4. for different time instances during which the full set of equations is solved without time-averaging technique. Between these instances, time averaging technique is applied for Navier-Stokes equations only. One could note several features of the discharge. The time evolution of current looks like almost chaotic one. However, one can distinguish several characteristic time zones. Current peaks corresponding to the growing part of HV voltage are due to “streamers” passing over the dielectric plate from HV electrode. Streamers, in general, are varied in length and life time. The magnitude of each current peak correlate well with the distance the streamer passes over the plate toward the symmetry axis. Examples of streamers evolution are presented in Fig.5. This behavior is typical for initial time period, when every next HV electrode operation cycle ($30\text{ }\mu\text{s}$) is not strongly influenced by changes in flow field. On later stages, heating of the air over the dielectric changes the air density, which, in general, increases the amplitude of one of the important quantity, E/n . In turn, increase in reduced electric field E/n results in faster ionization near the streamer head. As a result, more streamers pass full distance from the HV electrode to the axis of symmetry. It should be noted that positive-current streamer usually jumps over the portion of dielectric surface nearest to HV electrode

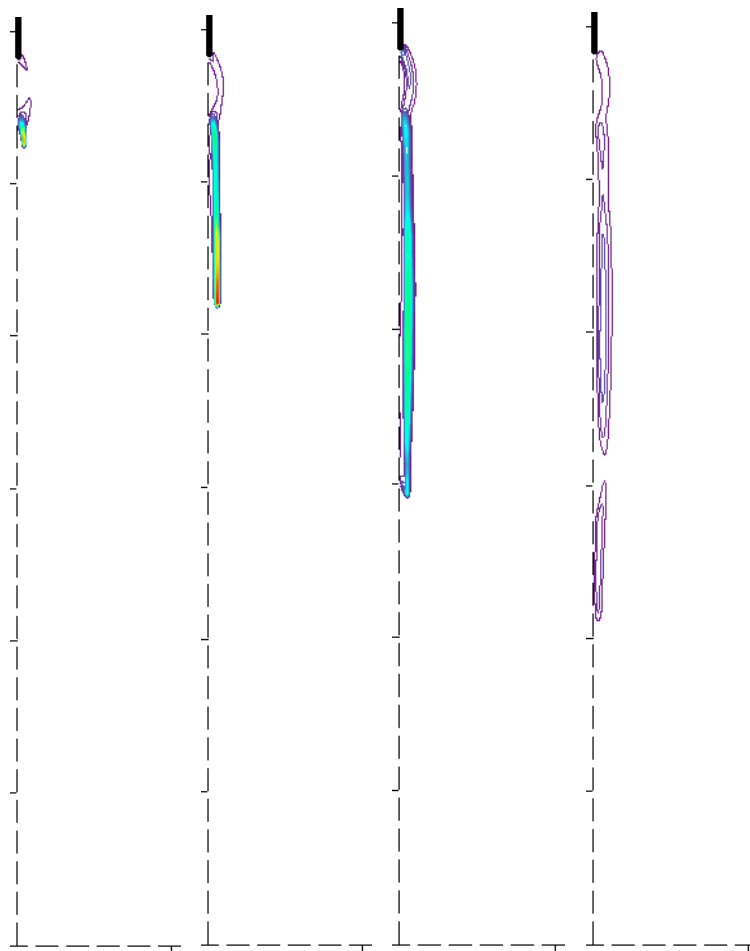


Fig.5. Ni field for the last streamer from Fig.4. $N_{\text{imax}}=3.9\cdot 10^{20}\text{ m}^{-3}$. Part of HV electrode is designated by thick black line. Dashed vertical line is the dielectric surface. Dashed horizontal line is axis of symmetry.

edge. In general, the discharge behavior depends not only on the instant applied voltage, but also on the distribution of electric potential on the surface. Typically, both ionization rates in the head of streamer and the length the streamer passes are determined by the local values of near-surface electric field. The latter, in turn, is determined by the distribution of the surface charge. The distribution of electric charge is quite non-uniform over the surface because it depends on surface charge deposited earlier. Therefore, anode-type operation mode is observed for HV electrode even if the applied voltage is negative relative to its ground-value. Similarly, cathode-type operation mode is observed for the HV electrode even if the applied voltage is positive relative to the ground value.

Examples of streamer passing over the dielectric surface are given in Fig.5. These pictures correspond to the last current peak from Fig.4. More exact, they correspond mainly to the growing part of the peak, which takes about 90 ns. First two positive-current streamers from Fig.4 pass the complete distance between electrode and the axis. Negative-current streamers (cathode-type operation mode for HV electrode) produce typically smaller plasma concentrations over the dielectric surface in comparison with the near-edge values of ion or electron concentrations.

The main question of this work is how the pulse-periodic discharge effects on the flow field. As found from calculations, the main effect of the discharge comes from the region near the electrode edge. Local maxima of both heat release and force are located either just top or just below the leading edge of HV electrode depending on the operation mode. As far as near-edge heat release is concerned, it can be considered as pulse-periodic power source making the main contribution to the fluid disturbance. The near-edge dynamic source appearing in equation (2) due to the electric charge acts always toward the wall, which could lead to the change in the pressure field near the wall. The influence of negative-current streamers (the electrode edge is not considered) is small. The influence of positive-current streamers on the flow is remarkable though it is less than those near the electrode edge. When positive-current streamer passes over the dielectric surface, two places of disturbances can be mentioned. First, the head of streamer is always the source of both heat and force. The force directs from the electrode toward the axis. Second, the bulk of air between

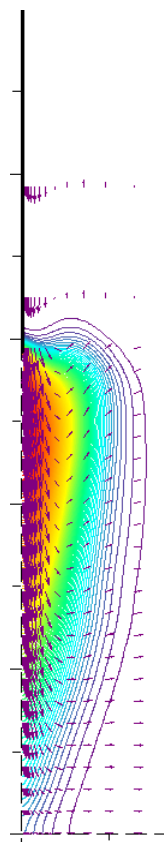


Fig.6. Temperature and velocity field at $t=1.5\text{ms}$ calculated with time-averaging technique. $T_{\text{max}}=778\text{K}$, $U_{\text{max}}=1.12\text{ m/s}$. HV electrode is shown by thick black line.

the quasi-neutral streamer body and the dielectric surface. This is cathode layer in which the force is directed mainly toward the wall. Combined effect of both heat release and electrostatic force is the vortex production over the plate. Example of long-term flow field obtained with time-averaged source-terms is shown in Fig.6. Note that instant flow field can be quite different from the time-averaged one.

3. Concluding remarks and future work

Direct fully self-consistent numerical simulation of the heat and dynamics effects of the sinusoidal surface dielectric barrier discharge is used to predict the flow field evolution under conditions closed to experimental ones described in the paper [1]. The preliminary results have shown that induced air flow is formed both by heated gas expansion (mostly isotropic factor) and the (vectorized) electrostatic body

force. The instant distributions of the gas velocity and temperature are highly non-uniform due to the strong non-uniformities of joule heat release, pressure gradient and body force.

It is important to outline that for conditions considered (as well as for very wide range of SDBD conditions) the joule heating power is much greater than the body force work power [4]. The detailed mechanism of the well-recognized streaming flow is the goal of our next steps of the study. The combined technique of the numerical simulation of time multi-scale evolution in plasma aerodynamics systems has been developed and successfully tested for the realistic configuration.

The qualitatively correlation with the experimental data presented in paper [1] has been demonstrated. The quantitative correlation will be the task of our next step efforts.

Acknowledgement

This work was partially supported by the Russian Science Foundation, grant No. 14-50-00124. The authors are grateful to Dr. I. Moralev and to Dr. V. Soloviev for fruitful discussions.

References

- [1] M Taglioli, A Shaw, A Wright, B FitzPatrick, G Neretti, P Seri, C A Borghi and F Iza, “EHD-driven mass transport enhancement in surface dielectric barrier discharges”, *Plasma Sources Sci. Technol.* 25 (2016) 06LT01 (5pp), doi:10.1088/0963-0252/25/6/06LT01e
- [2] Bityurin V., Bocharov A., and Popov N. “Numerical Simulation of the Discharge in Supersonic Flow Around a Sphere”, Paper 2007-0223, Proc. 45th AIAA Aerospace Sciences Meeting & Exhibit, 5-8 January 2007, Reno, NV.
- [3] V. A. Bityurin, A. N. Bocharov, and N. A. Popov, “A High_Frequency Discharge on a Dielectric Surface”, *High Temperature*, 2011, Vol. 49, No. 5, pp. 758–761
- [4] V. A. Bityurin, *Dynamics and Heat Release Effects in Magneto-Plasma Aerodynamics*, In: WSMFA 16, Moscow, JIHT, 2016